UNICA UNIVERSITÀ DEGLI STUDI DI CAGLIARI

This is the Author's accepted manuscript version of the following contribution:

M. López-Suárez, C. Melis, L. Colombo and W. Tarantino,

"Multiscale Modelling of Resistive Switching in Gold Nanogranular Films"

***2023 IEEE Nanotechnology Materials and Devices Conference (NMDC)*, Paestum, Italy, 2023, pp. 798-802**

The publisher's version is available at:

http://dx.doi.org/**10.1109/NMDC57951.2023.10344176**

When citing, please refer to the published version.

This full text was downloaded from UNICA IRIS https://iris.unica.it/

Multiscale modelling of resistive switching in gold nanogranular films*

Miquel López-Suárez, Claudio Melis, Luciano Colombo, Walter Tarantino

***Abstract*— Metallic nanogranular films display a complex dynamical response to a constant bias, typically showing up as a resistive switching mechanism which, in turn, could be used to create electrical components for neuromorphic applications. To model such a phenomenon we use a multiscale computational approach blending together (i) an ab initio treatment of the electric current at the nanoscale, (ii) a molecular dynamics approach dictating structural rearrangements, and (iii) a finite-element solution of the heat equation for heat propagation in the sample. We also consider structural changes due to electromigration which are modelled on the basis of experimental observations on similar systems. Within such an approach, we manage to describe some distinctive features of the resistive switching occurring in a nanogranular film and provide a physical interpretation at the microscopic level.**

I. Introduction

The ability of engineering materials down to the atomic scale reached in the last decades has open the door to an unprecedented tailoring of their physical properties. In turn, newly synthesized nanostructured materials present features bearing the potential ofunforeseen technological applications. This is the case, for instance, of thin cluster-assembled gold films, which present a rich dynamical non-Ohmic response to an external bias that could be exploited, as suggested in Refs. [1-5], in the fabrication of unconventional computing hardware components. More specifically, even under a constant bias, the electrical resistance of such systems can suddenly change over macroscopic scales giving rise to what are usually called resistive switching (RS) events. The microscopic mechanisms behind them are still far from being identified and fully characterized, partially due to a lack of specialized theoretical tools for a quantitative analysis of the RS phenomenon.

In this paper we will investigate the conductivity of cluster-assembled Au films as a temperature-dependent tensor field, reflecting the anisotropic and non-homogeneous nature of the sample at nanometer scale. In addition, we shall argue that in Au nanogranular films (ng-film) the electrical conductivity sensibly depends as well on the current flowing within the sample through electromigration (EM) effects.

*Research supported by Fondazione CON IL SUD (Grant No. 2018-PDR-01004).

M. López-Suárez, C. Melis, L. Colombo, W. Tarantino are with the Department of Physics, University of Cagliari, Cittadella Universitaria, 09042 Monserrato (Ca) ITALY (e-mail: claudio.melis@dsf.unica.it).

.

II. Phenomenolgy

Au clusters of a few nanometers in diameter can be produced in gas phase and gently deposited on a substrate to form, layer after layer, a ng-film. By growing the sample between two electrodes, one can probe its responseto an external electrical bias [6]. Besides the usual insulating/metal transition occurring around the percolation threshold, Au ng-films are found to present a rather complex non-Ohmic response, even when the film has grown far from that threshold [1-3].

In the simplest situation of a constant applied voltage, the response of the Au ng-film is highly dynamical. More specifically, upon application of a sufficiently high bias, the initially low and constant resistance suddenly increasesto a much higher (up to two orders of magnitude) value. After this initial phase, hereafter referred to as "sample activation", RS events show up, appearing as sudden jumps of the sample resistance; while the jump series occurs over a macroscopic scale, the jump itself is characterized by a much shorter time scale.

Resistance jumps can occur in either directions: to higher as well as to lower values (i.e. they show up as reversible processes). Furthermore, recurrent resistance values have been measured over long observationalperiods. Also, the higher the voltage of the external bias the more frequent the jumps are. Finally, sample activation is permanent: after the bias is switched off, an activated sample will show right away resistive switching events the next time a bias is again switched on.

III. Multiscale modeling

The electrical response of an Au ng-film is calculated by a multiscale approach. To have a direct connections with the experiments and, more generally, with macroscopic observables, we start from a set of equations that allows us to determine the sample resistance and temperature; then, some of the parameters there appearing are determined via atomistic simulations, where possible, or modeled on some experiments.

More specifically, at the macroscopic scale, a set of classical equations (namely, Fourier heat equation and Kirchhoff circuit laws coupled via Joule heating) are numerically solved on a uniform grid, leading to the estimation of both electrical resistance and temperature of Au films. At the microscopic scale, instead, molecular dynamics (MD) simulations and *ab initio* total-energy calculations are used to estimate the value of electrical conductivity that enters into the macroscopic equations.

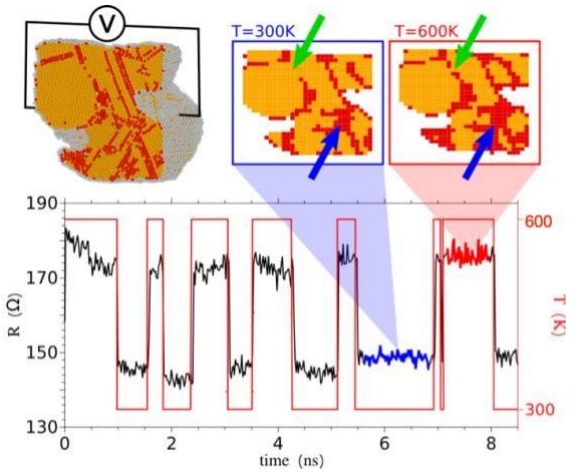

Figure 1. Modulation of the local resistance (black line and left scale in the bottom panel) of a ng-Au snippet under bias (top left panel) resulting from a random time-variation of its local temperature (red line and right scale in the bottom panel). The top right panels: the cluster-cluster junction marked by the green (blue) arrow undergoes (does not undergo) temperature-induced structural modifications (yellow and red areas indicate crystalline and amorphous regions, respectively).

A. The macroscopic conduction model

Because of the structural changes occurring at the cluster length-scale and triggered by local variations of both temperature and current (see Secs. III B and C), the key physical quantities to focus on are the temperature and current fields. Their interplay can be formalized as a macroscopic thermistor problem [7], which reads as

$$\rho\, C\, (\partial T/\partial t) = \mathrm{div}\,[\kappa \cdot \mathrm{grad}(T)] + \mathbf{I} \cdot \sigma \cdot \mathbf{I} \qquad (1)$$

where ρ and C are scalar quantities, respectively representing the mass density and the specific heat of the ng-film; in this equation, vector and tensor quantities are indicated by bold symbols: κ and σ respectively are the thermal and electric conductivity tensor, while $\mathbf{I}$ is the electric current vector field obeying the constraint $\mathrm{div}(\mathbf{I})=0$. The complex microstructure of the ng-film is fully exploited by the ρ, C, κ and σ parameters.

The numerical solution of (1) is found by a finite element method and, therefore, the above physical parameters are referred to each mesh cell (which typically contain several Au clusters). In fact, ρ and C are kept constant throughout the simulated samples since it is experimentally reported that no sizeable changes are observed in the overall ng-film topography (although the cluster-cluster interface structure indeed undergoes evolution, as commented above). On the other hand, κ and σ conductivities are considered site-dependent. Finally, as we are dealing with a metallic system, by the Widemann-Franz (WF) law it holds $\kappa = LT\,\sigma$, where L is the Lorenz number. Therefore, σ actually encodes whatever change happens at the microscopic scale.

B. Temperature-induced variations of local resistance

The present microscopic picture is based on the atomistic samples of Au ng-films generated by the large-scale MD simulations reported in [8], where an embedded-atom model potential [9] was used to describe interatomic interactions. Temperature modulation (see below) was operated by a Nosé-Hoover thermostat, while keeping track of any structural evolution through the collected atomic trajectories. As argued in [6,10], we neglected the contribution of quantum phenomena (electron hopping and tunneling) in evaluating the resistance and just focus on atomic-scale structural changes.

To investigate how temperature variations affect the resistance R(T) within the Au ng-film, we at first cut out from the computer-generated samples a few snippets with size about 15 nm and put them under bias (Fig.1, top left panel). Next, by a random time-modulation of their temperature between 300K and a higher value, we followed their microstructural evolution and calculated the associated R(T) by the previously developed *ab initio* tool [8]. The accurate evaluation of the ballistic electronic transport was obtained by combining ab initio density functional theory with nonequilibrium Green's functiontechnique, as detailed in [8] and references therein. We emphasize that the characteristic size of the irregularities ina nanogranular film closely aligns with the electron mean free path in the corresponding crystalline phase, whichamounts to 37.5 nm for gold (Au).

The typical observed behavior for a temperature modulation in between 300K and 600K is reported in Fig.1 which provides compelling evidence that local RS events are effectively induced by a temperature variation. We propose the following concept: altering the temperature, whether it is increased or decreased, leads to neat and reversible local conduction variations. At the microscopic level, we recognize some structural rearrangements which we generically label as transitions from more (crystal-like) to less (amorphous-like) ordered states. The current temperature range investigated, which spans from 400 K to 600 K, effectively inhibits the fusion of nano-sized gold particles into larger agglomerates.

The observed R(T) behavior resulting from our simulations was encoded as

$$R(T) = R_0\,[1 - \theta(T-T_{thr})\,\Delta] \qquad (2)$$

where R_0 is the room temperature resistance, T_{thr} (in between room and melting temperatures) is the threshold temperature for triggering structural modifications, Δ indicates the magnitude in change of resistance, and θ is the Heaviside step function. Equation 2 effectively quantifies the sudden change of resistance that might occurwhen the temperature exceeds T_{thr}. As shown in Fig.1 (top right panel), this behavior is linked to reversible amorphization/recrystallization cycles occurring at cluster-cluster interfaces.

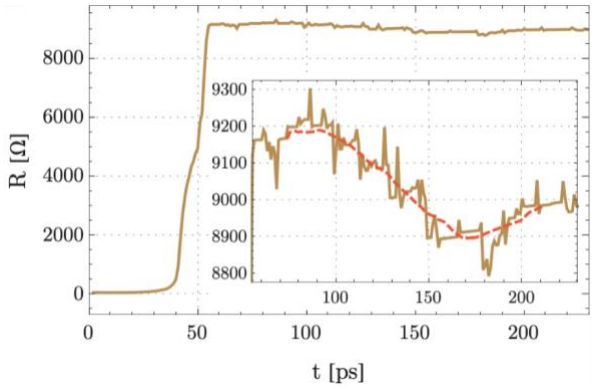

Figure 2. Resistance of a simulated Au ng-film. The inset plot shows a zoom-in of the resistance after the activation phase. Dashed line in the inset represents the time-average resistance.

The resistance properties dictated by (2) feed the macroscopic model outlined in (1) in two ways: first of all, they directly determine the electrical conductivity term, which is essentially the inverse of R(T); furthermore, as already commented, they enter in the determination of the thermal conductivity through the application of the WF law. In particular, this implies that the estimate of thethermal conductivity of a given cell is actually provided by its electrical counterpart, which effectively encodes any "microscopic" feature (in this context referring to changes at the length scale of a single cell). In contrast to conventional multiscale methods, our approach does not require computing such information at each timestep of resolution of (1). Instead, we employ theoretical tools and existing experimental data to map σ with respect to temperature and current once and for all. This mapping is then used in the resolution of the interconnected system of equations.

C. Current-induced variations of local resistance

There is experimental evidence of a certain EM effect in nanostructured metallic systems; the present ng-films are actually not that far in structure and similar in chemical composition and, therefore, it is quite reasonable to suppose that the same EM effect also occurs in the experiments we are referring to [1-4,11-13]. However, unlike the thermal issue connecting T to R, we cannot run direct simulations on the EM effect (which connects R to I) and so we use a simple model to encode it in our framework. More specifically, we assume that, under a suitably high voltage, EM effects lead to a reduction of the contact area between two Au clusters, to the point where a disconnection phenomenon between the two clusters possibly occurs [12,14]. In order to account for the structural inhomogeneity of Au ng-film, we need to allow junctions to independently shrink/break in any possible direction (even different from the direction of applied voltage).

The observed EM effects are encoded in just two macroscopic parameters, namely: (i) an activation current I_a is defined such that for any value $I>I_a$ the effective contact area A_c of the junction shrinks, and (ii)a shrinking parameter β is introduced such that, whenever the above activation condition is reached, the effective contact area is reduced to A_c/β. The magnitude of the required bias for achieving a noticeable EM effect typically falls within the range of 0.2-0.4 V.

IV. Results and Discussion

The theoretical device of Sec. III can hardly be implemented on a parameter set straightforwardly fixed as discussed above: it would simply be too computationally demanding. Rather, we operate a reasonable rescaling of such values so as to show some relevant phenomena with a reasonable effort. More specifically, the parameters entering in (1) were randomly assigned cell-by-cell in the intervals $0<R_0<250\Omega$, $300K<T_{thr}<340K$, and $0<\Delta<0.2$. Next, local activation currents were randomly extracted from the $0.9\mu A<I_a<1.08\mu A$ and $2.0\mu A<I_a<2.4\mu A$ intervals, while just one $\beta=5$ factor has been used. For the remaining model parameters entering in (1), we used $\rho C=0.016 kg^2K^{-1}m^{-1}s^{-2}$ and $L=2.44x10^{-8}V^2K^{-2}$. Time evolution was discretized by a time-step as short as 1ps.

To numerically solve the thermistor model, we considered finite-element mesh corresponding to 80x80x4 cubic cells of side d=15nm: any Au ng-film was accordingly identified by a set of parameters characterizing each of its single cells. Finally, the Joule heat produced in the Au ng-film was dissipated through all boundaries of the simulated sample, while we set the initial temperature at T=300K for all cells. Finally, the applied voltage ramped from zero to 0.014V during the first 30ps and then kept constant. This setup generates an electric field close to the experimental one [1,2].

In Fig.2 we report the calculated evolution of the resistance of a simulated Au ng-film. We can distinguish two regimes, different by orders of magnitudes as for the actual resistance values: negligibly small and very high, respectively. Eventually, the resistance stabilizes, although, on a short time scale, some variations are still present as shown in the inset. By analyzing the microstructural evolution of each single cell during the simulation, we realized that the initial regime is dominated by EM effects. They lead to an extensive deterioration of the sample, as shown in the t op row of Fig.3, where the the conductivity σ_x along the bias direction (hereafter labelled as *x*) is reported: while uniform at first, it eventually appears largely affected once that the EM activation threshold is exceeded.

According to our analysis, nearly a third of the cells experienced reduction phenomena of contact areas along the bias direction; in most cases (about 80%) this turned into (at least) one broken connection. As the current trying to find its way through such an inhomogeneous medium, interfaces normal to directions other than the bias one (hereafter referred to as transverse directions) were as well largely affected by EM. As a matter of fact, nearly 12% of cells experienced reduction of contact areas along a transverse direction. Nevertheless, just few cells (no more than 1.5%) wereleft completely insulating, i.e. with no current flowing in any direction. The voltage was chosen to be not high enough to actually break the sample and, therefore,

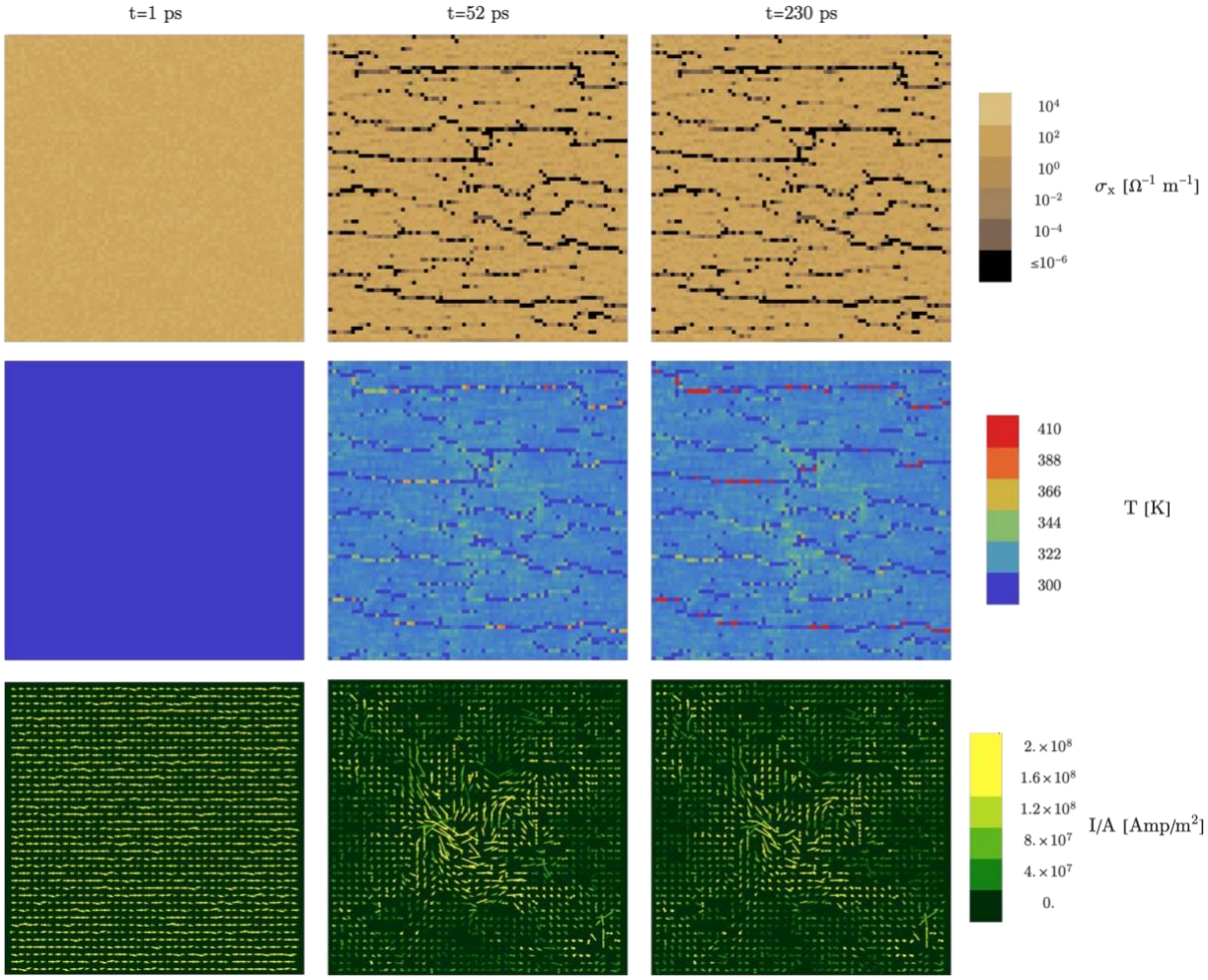

Figure 3. Conductivity σ_x along the *x* bias direction (first row), temperature T (second row), and current density vector I/A (third row) inside the simulated Au ng-film at three different times. The first snapshot is taken at the very first time step of the simulation when the sample is at room temperature, its conductivity is high and the current flows rather uniformly fro m one electrode to the other; the second snapshot corresponds to the end of the deterioration phase induced by electromigration effects; the last snapshot (taken at t he very end of the simulation) shows that structural changes occurring after the activation phase are much less visible. Arrows in the third row represent the projected current; to better visualize the current field, both the length and the color of the arrows represent its inten sity.

EM effects eventually become negligible. At this stage, thermal effects dominate, leading to some noisy variations of the film resistance and generating its more stable variations shown in the inset of Fig.2.

Consistently with the two regimes found for the resistance, the calculated time evolution of the sample average temperature (here not shown) is again a two- step process: initially it grows at a high rate (since the overall resistance is still comparatively low), but then its growth is slowed down by the increase in the resistance described above. More intriguing is the case of the local temperature whose map is plotted in the second row of Fig.3: regions with higher resistance tend to become hotter. This is due to the fact that, as the electrical conductance locally lowers, so does the thermal one (κ and σ are proportional through the Wiedemann-Franz law): ultimately, because of the slow heat dissipation rate, overheating occurs.

In the last row of Fig.3 a comparison is presented between the current field I/A (where A is the sample cross section) before (left panel) and after (middle and right panels) the Au ng-film deterioration. While initially the current flow is basically uniform, preferred percolative-like paths eventually emerge upon EM- induced deterioration. This is due to the fact that, although only few cells now result to be totally (i.e. isotropically) insulating, the active current paths result to be shaped along meandering tracks, since as many as 1/3 of the cells do not let it to straightforwardly proceed along the bias direction.

V. Conclusions

We provided evidence that temperature-induced and current-induced variations of resistance are distinct and consequential phenomena, with thermal effects being relevant only after EM has deteriorated the sample. It seems therefore reasonable to establish a direct link

between the deterioration phase observed in our simulations and what is experimentally referred to as the "sample activation" [6]: in both cases the increase in resistance represents the necessary pre-condition for resistive switching events to emerge. As soon as electromigration no longer plays a role, thermally activated variations of the local resistance are found in quantitative agreement with experiments: the average resistance of the simulated samples varies from 9200 Ωto 8900 Ω, remarkably close to the measurements reported in [1], which range from 9900 Ω to 9300 Ω.The calculated time scale of such microscopic variations is of the order of 100ps and, therefore, they macroscopically show up as sudden jumps as reported in experiments. Finally, by using the present multiscale modelling a piece of explanation of the reason why RS events emerge on deteriorated samples comes from the analysis of the current field: the EM-induced deterioration leads to the emergence of a pattern of current which does not flow uniformly throughout the Au ng-film, but it rather follows some preferred paths. Even slight changes occurring on a single path can have macroscopic effects: the switching of just a few cells to a high resistive state makes that path no longer favorable and, in turn, this largely affects the resulting conduction regime.

Present results certainly motivate to extend our work in several directions: running larger scale (both of time and length) simulations in search of other key features of resistive switching in Au ng-films; exploring larger regions of the parameter space (also covering possible but-yet-to-explore experimental conditions); and, last but not least, apply the same methodology to other systems (sub-monolayer ng-films or more complex nanostructures, like nonocomposite ones).

REFERENCES

[1] M. Mirigliano, F. Borghi, A. Podestá, A. Antidormi, L. Colombo, P. Milani, "*Non-ohmic behavior and resistive switching of Au cluster-assembled films beyond the percolation threshold*", Nanoscale Advances **1**, 3119 (2019).

[2] M. Mirigliano, D. Decastri, A. Pullia, D. Dellasega, A. Casu, A. Falqui, and P. Milani, "*Complex electrical spiking activity in resistive switching nanostructured Au two-terminal devices*", Nanotechnology **31**, 234001 (2020).

[3] M. Mirigliano, B. Paroli, G. Martini, M. Fedrizzi, A. Falqui, A. Casu, and P. Milani, "*A binary classifier based on a reconfigurable dense network of metallic nanojunctions*", Neuromorphic Computing and Engineering **1**, 024007 (2021).

[4] C. Barone, M. Bertoldo, R. Capelli, F. Dinelli, P. Maccagnani, N. Martucciello, C. Mauro, S. Pagano, "*Electric Transport in Gold Covered Sodium Alginate Free Standing Foils"*, Nanomaterials, **11**, 565 (2021).

[5] C. Barone, P. Maccagnani, F. Dinelli, *et al.* "*Electrical conduction and noise spectroscopy of sodium-alginate gold-covered ultrathin films for flexible green electronics"*, Scientific Reports **12**, 9861 (2022).

[6] E. Barborini, G. Corbelli, G. Bertolini, P. Repetto, M. Leccardi, S. Vinati, and P. Milani, "*The influence of nanoscale morphology on the resistivity of cluster-assembled nanostructured metallic thin films*", New Journal of Physics **12**, 073001 (2020).

[7] S.N. Antontsev and M. Chipot, "*The thermistor problem: existence, smoothness, uniqueness, blowup*", SIAM Journal of Mathematical Analysis **25**, 1128 (1994).

[8] M. López-Suárez, C. Melis, L. Colombo, and W. Tarantino, "*Modeling charge transport in gold nanogranular films*", Physical Review Materials **5**, 126001 (2021). of overheating and potential damage to the entire sample.

[9] S.M. Foiles, M.I. Baskes, and M.S. Daw, "*Embedded-atom method for fcc metals Cu, Ag, Au, Ni, Pd, Pt, and their alloys*", Physical Review B **33**, 7983 (1986).

[10] W. Tarantino and L. Colombo, "*Modeling resistive switching in nanogranular metal films*", Physical Review Research **2**, 043389 (2020).

[11] B. Stahlmecke and G. Dumpich, "*Resistance behaviour and morphological changes during electromigration on gold nanowires*", Journal of Physics: Condensed Matter **19**, 046210 (2007).

[12] Z.M. Wu, M. Steinacher, R. Hber, M. Calame, S.J. van der Molen, and C. Schönenberger, "*Feedback controlled electromigration in four-terminal nanojunctions*", Applied Physics Letters **91**, 053118 (2007).

[13] S. Karim, K. Maaz, G. Ali, and W. Ensiger, "*Diameter dependent failure current density in gold nanowires*", Journal of Physics D: Applied Physics **42**, 185403 (2009).

[14] In the production of highly integrated devices, a practical solutionto tackle electromigration-induced degradation is the integration ofa feedback circuit. This circuit can gradually raise the sample's bias voltage until it reaches a predetermined resistance threshold, and once reached, it can effectively stabilize the voltage, thereby reducing the chances.